ANALYSIS OF SHOCK RELATIONS FOR STEADY POTENTIAL FLOW MODELS

B. SANDERSE AND B. KOREN

ABSTRACT. Potential flow models remain to be practically relevant, for both physical and numerical reasons. Detailed knowledge of their difference with rotational and viscous flow models is still important. In the present paper, this knowledge is reviewed and extended. Normal and oblique shock relations for the steady full potential equation and steady transonic small disturbance equation are derived. Among others, the deficiencies in conservation of mass and momentum across shock waves are analyzed in detail for these potential flow models. By comparison with the shock relations for the Euler equations guidelines are offered for the applicability of potential flow models in numerical simulations. Furthermore, the analytical expressions derived here may serve for verification of numerical methods.

1. INTRODUCTION

Given the immense progress in numerical methods for Euler and Navier-Stokes flow computations over the last three decades, potential flow models may seem to become obsolete. However, practically relevant potential flow simulations remain to exist, because numerical computations based on potential flow equations can provide quantitative answers in shorter wall-clock time compared to Euler and Navier-Stokes equations [2]. This makes the potential flow model very useful in design and optimization studies, encountered in for example the aircraft industry [3, 5]. Viscous corrections or coupling with Navier-Stokes codes extend their range of applicability while retaining most of the fast solution procedure (see e.g. [1]). For practical purposes, it is important to precisely know the differences between potential flow models on the one hand and Euler or Navier-Stokes flow models on the other hand. Further, for rigorous verification of potential flow models codes, it is important to have a broad and deep knowledge of potential shock relations.

In the present paper we focus on the capability of two compressible potential flow models, being the full potential equation (FPE) and the transonic small disturbance equation (TSD), to resolve steady shock waves as predicted by the Euler equations. A good knowledge of the differences between these models is important for, particularly, preliminary aircraft design in the high-subsonic, transonic and low-supersonic speed regimes. There is an ongoing interest in these designs from the viewpoint of fuel consumption and noise nuisance.

We complete this introduction by a short rehearsal of shock waves as weak solutions of partial differential equations and with the derivation of the well-known shock relations for the Euler equations. Subsequently, in sections 2 and 3 normal and oblique shock relations for the FPE and the TSD are derived and extensively compared with the corresponding Euler relations. Deficits in momentum and mass conservation are also analyzed. These analyses provide a complete description and overview of normal and oblique shocks in steady potential flow models.

1.1. **Weak solution of partial differential equations in conservative form.** A general two-dimensional formulation of a partial differential equation in conservative form can be written

(A) Discontinuity $\mathcal{D}$ and control volume $\mathcal{S}$.
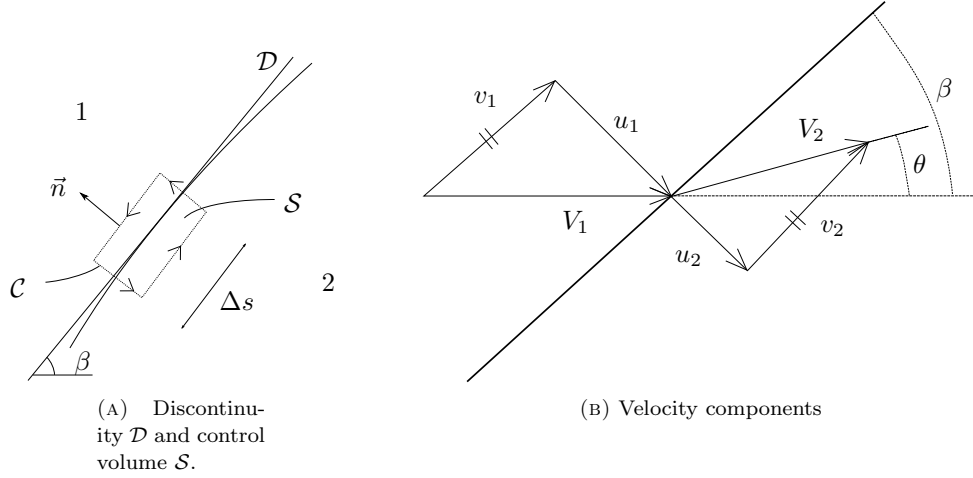
(B) Velocity components

FIGURE 1. Nomenclature for shock wave.

as

$$(1) \qquad\qquad F_x + G_y = 0,$$

or as

$$(2) \qquad\qquad \nabla \cdot \vec{A} = 0, \quad \text{with} \quad \vec{A} = \begin{pmatrix} F \\ G \end{pmatrix}.$$

To obtain weak solutions of (2) we consider a control volume $\mathcal{S}$ that embodies a discontinuity $\mathcal{D}$ (figure 1a) over which we integrate (2):

$$(3) \qquad\qquad \iint_{\mathcal{S}} \nabla \cdot \vec{A} \, \mathrm{d}S = 0.$$

Application of the divergence theorem gives

$$(4) \qquad\qquad \oint_{\mathcal{C}} \vec{A} \cdot \vec{n} \, \mathrm{d}C = 0.$$

With the thickness of the control volume approaching zero, we get

$$(5) \qquad\qquad \oint_{\mathcal{C}} \vec{A} \cdot \vec{n} \, \mathrm{d}C = \begin{pmatrix} F \\ G \end{pmatrix}_1 \cdot \vec{n}_1 \Delta s + \begin{pmatrix} F \\ G \end{pmatrix}_2 \cdot \vec{n}_2 \Delta s = 0.$$

Taking into account the opposite sign of the unit normal vectors $\vec{n}_1$ and $\vec{n}_2$ we can write the following jump relation:

$$(6) \qquad\qquad (F_2 - F_1) \tan \beta = (G_2 - G_1),$$

where β is the wave angle (figure 1a).

1.2. **Summary of shock relations for the Euler equations.** The steady Euler equations in two dimensions read

$$(7) \qquad\qquad \begin{pmatrix} \rho u \\ p + \rho u^2 \\ \rho u v \\ \rho u H \end{pmatrix}_x + \begin{pmatrix} \rho v \\ \rho v u \\ p + \rho v^2 \\ \rho v H \end{pmatrix}_y = 0,$$

with ρ, p, u and v denoting density, pressure and velocity components in x- and y-direction, respectively. H denotes the total enthalpy, which is related to the primitive quantities as $H = \frac{\gamma}{\gamma-1}\frac{p}{\rho} + \frac{1}{2}(u^2 + v^2)$, in case of a perfect gas, with γ the ratio of specific heats. Applying equation (6) for steady one-dimensional shocks, the following jump relations are found:

$$(8) \qquad [\rho u] = 0, \qquad [p + \rho u^2] = 0, \qquad [\rho u H] = 0,$$

where $[.] = (.)_2 - (.)_1$. The well-known corresponding relation between pre- and post-shock Mach numbers, M_1 and M_2 respectively, reads

$$(9) \qquad M_2^2 = \frac{2 + (\gamma - 1)M_1^2}{2\gamma M_1^2 - (\gamma - 1)},$$

and the corresponding pressure and density jumps over the shock are

$$(10) \qquad \frac{p_2}{p_1} = \frac{2\gamma M_1^2 - (\gamma - 1)}{\gamma + 1},$$

$$(11) \qquad \frac{\rho_2}{\rho_1} = \frac{(\gamma + 1)M_1^2}{2 + (\gamma - 1)M_1^2}.$$

For steady two-dimensional shocks (oblique shocks) in Euler flows the following known relation exists:

$$(12) \qquad \tan\theta = 2\cot\beta\frac{M_1^2\sin^2\beta - 1}{M_1^2(\gamma + \cos 2\beta) + 2},$$

where β is the wave angle and θ the deflection angle, see figure 1b.

2. Full potential equation

The FPE in two dimensions is given by:

$$(13) \qquad (\rho\phi_x)_x + (\rho\phi_y)_y = 0,$$

where ϕ is the potential whose gradient is the velocity vector, $\vec{V} = \nabla\phi$, meaning that the velocity field is irrotational. Equation (13) expresses conservation of mass, like the first equation of (7). Besides irrotationality, the potential formulation is often accompanied by the assumptions of homentropy and homenthalpy. The momentum equations are dropped and the remaining equations are algebraic only:

$$(14) \qquad \frac{p}{\rho^\gamma} = \text{constant} \qquad \text{(homentropy)},$$

$$(15) \qquad \frac{\gamma}{\gamma - 1}\frac{p}{\rho} + \frac{1}{2}(u^2 + v^2) = \text{constant} \qquad \text{(homenthalpy)}.$$

By combining the homenthalpic and homentropic conditions, the density and pressure can be related to the Mach number as:

$$(16) \qquad \frac{p_0}{p} = \left(\frac{\rho_0}{\rho}\right)^\gamma = \left(1 + \frac{\gamma - 1}{2}M^2\right)^{\frac{\gamma}{\gamma-1}},$$

where ρ_0 and p_0 are the total density and pressure. The FPE formulation based on equations (13) and (16) conserves mass and energy across shocks, but not momentum. Other formulations, which for example conserve mass and momentum but not energy, have also been suggested (see e.g. [4, 7]) but will not be considered here. In fact, the shock relations for the mass-momentum FPE model are closer to the shock relations of the Euler equations than those of the mass-energy FPE model. However, the advantage of the mass-energy FPE model is that only a single scalar differential equation has to be solved, which is not the case for the mass-momentum FPE model.

As is well known, the homenthalpic condition (15) is also valid for the steady Euler equations if the inflow is homenthalpic. The main error in the full potential formulation is therefore introduced by the assumption of homentropy, which is linked to the irrotationality condition via Crocco's theorem. The entropy error can be derived by considering the increase in entropy over normal shocks that satisfy the Euler equations. In terms of the perfect-gas entropy quantity $z = \ln(p/\rho^\gamma)$ it holds:

$$(17) \qquad e^{[z]} = \frac{p_2}{p_1}\left(\frac{\rho_1}{\rho_2}\right)^\gamma.$$

Substituting equations (9)-(11) and expanding in a Taylor series around $M_1 = 1$ leads to:

$$(18) \qquad [z] = \frac{16}{3}\frac{\gamma(\gamma-1)}{(\gamma+1)^2}(M_1-1)^3 + \mathcal{O}\left((M_1-1)^4\right).$$

Hence, the error made by assuming $z_1 = z_2$ in the FPE model is of third order in $M_1 - 1$.

The relative error in momentum conservation across a normal FPE shock can be written as:

$$(19) \qquad \frac{[p+\rho u^2]}{p_1 + \rho_1 u_1^2} = \frac{1+\gamma M_2^2}{1+\gamma M_1^2}\left(\frac{1+\frac{\gamma-1}{2}M_2^2}{1+\frac{\gamma-1}{2}M_1^2}\right)^{\frac{-\gamma}{\gamma-1}} - 1,$$

where equation (16) has been used to relate p and ρ to the Mach number. In the next section we proceed by deriving a relation between M_2 and M_1 for the FPE.

2.1. **Normal shock relations.** To derive steady normal shock relations for the FPE we return to equation (6) and figure 1a. For a normal shock wave we have $\beta = \pi/2$, so

$$(20) \qquad [F] = 0.$$

For the FPE $F = \rho u$, hence

$$(21) \qquad \rho_2 u_2 = \rho_1 u_1.$$

Considering a perfect gas, the velocity u is rewritten in terms of the Mach number as

$$(22) \qquad u = M\sqrt{\frac{\gamma p}{\rho}} = M\sqrt{\gamma\frac{p_0}{\rho_0}\frac{p}{p_0}\frac{\rho_0}{\rho}} = M\sqrt{\gamma\frac{p_0}{\rho_0}}\left(1+\frac{\gamma-1}{2}M^2\right)^{-1/2}.$$

With (16) and (22), equation (21) yields then:

$$(23) \qquad \boxed{\left(1+\frac{\gamma-1}{2}M_1^2\right)^{\frac{-(\gamma+1)}{2(\gamma-1)}}M_1 = \left(1+\frac{\gamma-1}{2}M_2^2\right)^{\frac{-(\gamma+1)}{2(\gamma-1)}}M_2.}$$

This is the FPE-analogue of equation (9). It is not possible to derive an explicit expression for M_2 as a function of M_1 for general γ. A numerical method is needed to obtain M_2 for given M_1, see e.g. [6]. A graph of M_2 as a function of M_1 according to equation (23), for $\gamma = \frac{7}{5}$, is given in figure 2. Like in shock relation (9) for the Euler equations, M_2 and M_1 are also interchangeable for the FPE model, i.e., (23) is symmetric with respect to the line $M_2 = M_1$.

It can be observed that the shocks satisfying the FPE are stronger than shocks satisfying the Euler equations. In order to analyze the error with respect to the Euler solution, we make a series expansion of both equations (9) and (23) around $M_1 = 1$, yielding:

$$(24) \qquad M_2^{\text{Euler}} = 1 - (M_1-1) + \frac{3\gamma-1}{\gamma+1}(M_1-1)^2 + \mathcal{O}\left((M_1-1)^3\right),$$

$$(25) \qquad M_2^{\text{FPE}} = 1 - (M_1-1) + \frac{\frac{5}{3}\gamma-1}{\gamma+1}(M_1-1)^2 + \mathcal{O}\left((M_1-1)^3\right),$$

hence

$$(26) \qquad M_2^{\text{Euler}} - M_2^{\text{FPE}} = \frac{\frac{4}{3}\gamma}{\gamma + 1}(M_1 - 1)^2 + \mathcal{O}\left((M_1 - 1)^3\right).$$

In contrast to the error in entropy, the error in post-shock Mach number is second order near $M_1 = 1$. Graphically this means that the slopes of the Euler and FPE graphs are equal at $M_1 = 1$ but the curvatures are not, see figure 2.

The relative error in momentum conservation, equation (19), can now be calculated. It is shown in figure 3 for $\gamma = \frac{7}{5}$ (the TSD results, also depicted here, will be derived in section 3). It can be seen that $[p + \rho u^2] > 0$, meaning that the FPE leads to a *gain* in momentum across the shock. By using equation (25), including higher order terms, we can make the following Taylor expansion of equation (19):

$$(27) \qquad \frac{[p + \rho u^2]}{p_1 + \rho_1 u_1^2} = \frac{16}{3}\frac{\gamma}{(\gamma + 1)^3}(M_1 - 1)^3 + \mathcal{O}\left((M_1 - 1)^4\right).$$

The relative error in momentum conservation is of third order, like the entropy error. Note that the two errors are related as:

$$(28) \qquad [z] = (\gamma^2 - 1)\frac{[p + \rho u^2]}{p_1 + \rho_1 u_1^2} + \mathcal{O}\left((M_1 - 1)^4\right).$$

Finally we note that, in the past, full potential flow models have been implemented in non-conservative form (see e.g. [2] and references therein). In such a form a mass conservation error (an effective mass source) is introduced at shocks, which has - nevertheless - accidentally led to better agreement with experimental data.
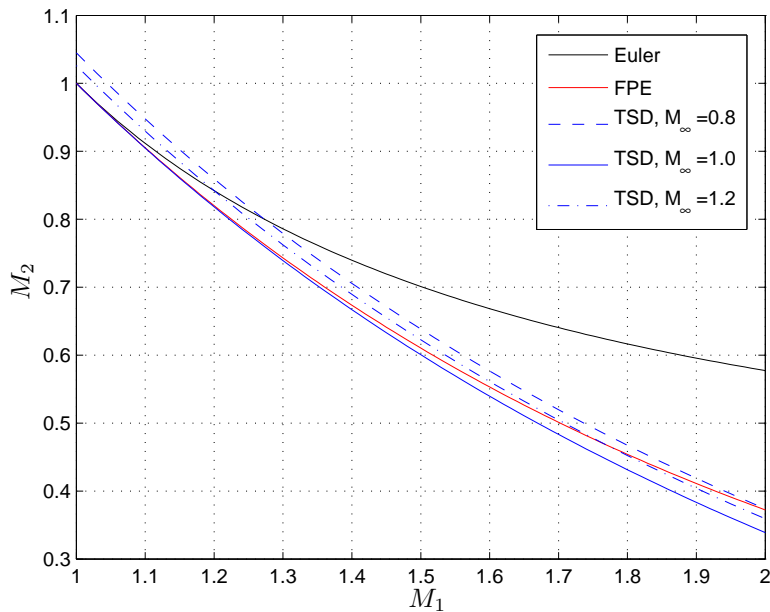

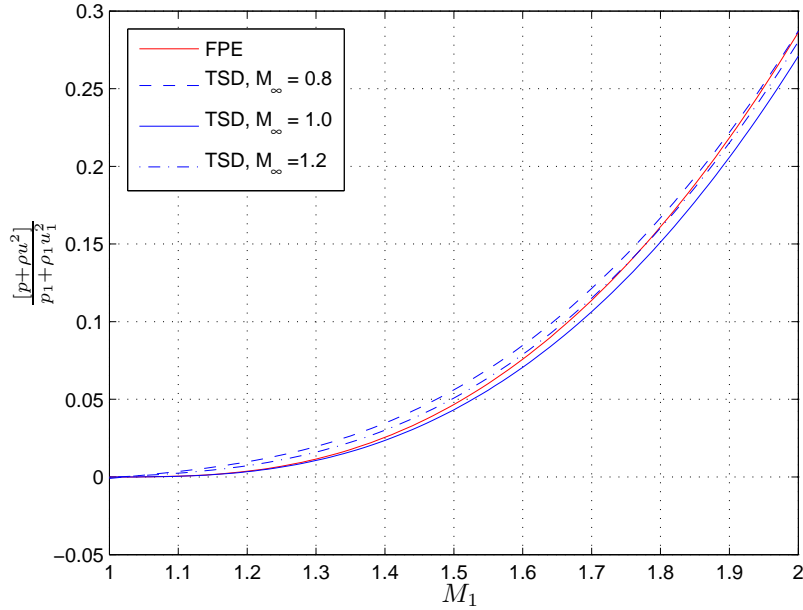FIGURE 2. Pre- and post-shock Mach number relations for the Euler equations, FPE and TSD, $\gamma = \frac{7}{5}$.

FIGURE 3. Relative momentum error for FPE and TSD, $\gamma = \frac{7}{5}$.

2.2. **Oblique shock relations.** For oblique shocks described by the Euler equations the momentum equation in a direction tangential to the shock can be used to show that

$$[v] = 0. \tag{29}$$

In flows governed by the full potential equation the momentum equations have been dropped. The normal component of the momentum flux is not conserved across a shock, as was just observed. The tangential component is still conserved though, as can be shown by integrating the irrotationality condition $\nabla \times \vec{V} = 0$:

$$\iint_{\mathcal{S}} \nabla \times \vec{V} \mathrm{d}S = \int_{\mathcal{C}} \vec{V} \cdot \mathrm{d}\vec{l} = 0, \tag{30}$$

from which it follows that $v_2 = v_1$. With mass conservation it then follows that $\rho_2 u_2 v_2 = \rho_1 u_1 v_1$. Hence, whereas the FPE model does not conserve normal momentum, it does conserve tangential momentum. This difference between conservation of normal and tangential momentum has already been noticed by Van der Vooren and Slooff [7].

In a direction normal to the shock (23) still holds, albeit with $M_{n,1}$ and $M_{n,2}$ instead of M_1 and M_2. To find the relation with M_1 and M_2, we need the definitions for the wave angle β and deflection angle θ (see figure 1b):

$$\frac{u_1}{v_1} = \tan \beta, \tag{31}$$

$$\frac{u_2}{v_2} = \tan(\beta - \theta). \tag{32}$$

With these definitions the pre-shock and post-shock Mach numbers normal to the shock follow as:

$$(33) \qquad M_{n,1} = M_1 \sin\beta,$$

$$(34) \qquad M_{n,2} = M_2 \sin(\beta - \theta).$$

From equations (21), (29) and (31) it follows that:

$$(35) \qquad \frac{u_2}{u_1} = \frac{\rho_1}{\rho_2} = \frac{\tan(\beta - \theta)}{\tan\beta}.$$

Expressing the pre- and post-shock densities ρ_1 and ρ_2 in terms of the Mach number by using equation (16) we find

$$(36) \qquad \boxed{\frac{\tan(\beta - \theta)}{\tan\beta} = \left(\frac{1 + \frac{\gamma-1}{2}M_{n,1}^2}{1 + \frac{\gamma-1}{2}M_{n,2}^2}\right)^{\frac{-1}{\gamma-1}}.}$$

This equation, together with (23) for the relation between $M_{n,1}$ and $M_{n,2}$, is the FPE analogue of equation (12). Given a supersonic flow with a certain $M_{n,1}$ and a deflection angle θ, the oblique shock-wave angle β can now be computed, if existent. The FPE relation between θ and β is shown in figure 4 for different pre-shock Mach numbers, and compared to the oblique shock relations for the Euler equations. As for the Euler equations, three different possibilities occur depending on the deflection angle:

(1) $\theta < \theta_{\max}$: two solutions. The 'weak' solution, i.e., the solution with the smallest β, normally occurs in practice.
(2) $\theta = \theta_{\max}$: one solution.
(3) $\theta > \theta_{\max}$: no solution; the shock wave is detached.

We observe that, considering weak solutions at a certain M_1 and θ,

$$(37) \qquad \beta^{\text{FPE}} \leq \beta^{\text{Euler}},$$

which is to be expected since the shocks predicted by the FPE are stronger. The agreement between the FPE and Euler relations improves with decreasing Mach number and decreasing deflection angle.

3. Transonic small disturbance equation

3.1. Normal shock relations.
The transonic small disturbance equation (TSD) in two dimensions is given by:

$$(38) \qquad \left(1 - M_\infty^2 - (\gamma + 1)M_\infty^2\varphi_x\right)\varphi_{xx} + \varphi_{yy} = 0,$$

where φ is the non-dimensional disturbance potential; $\varphi_x = u/V_\infty - 1$, with V_∞ the free-stream flow speed. In the derivation of this equation it is assumed that perturbations of the free-stream flow are small, which is typically valid for slender bodies at small angle of attack. Equation (38) is hyperbolic if

$$(39) \qquad \varphi_x > \frac{1 - M_\infty^2}{(\gamma + 1)M_\infty^2}.$$

This condition can be expressed solely in Mach numbers by writing the disturbance velocity φ_x in terms of the Mach number, similarly to equation (22), but now also using free-stream values besides stagnation values:

$$(40) \qquad u = M\sqrt{\frac{\gamma p}{\rho}} = M\sqrt{\gamma\frac{p_\infty}{\rho_\infty}\frac{p}{p_0}\frac{p_0}{p_\infty}\frac{\rho_0}{\rho}\frac{\rho_\infty}{\rho_0}}.$$
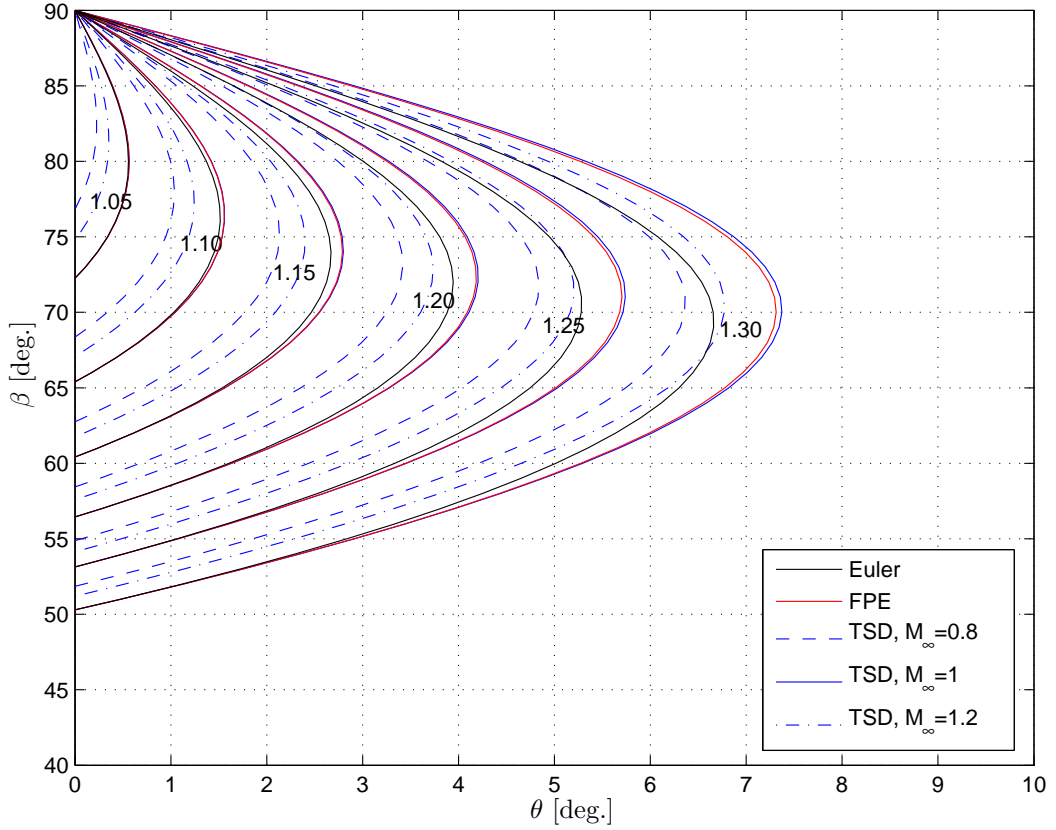
FIGURE 4. Oblique shock-wave properties for the Euler equations, FPE and TSD for different M_1, $\gamma = \frac{7}{5}$.

With the homentropic relations (16) this leads to the following requirement for hyperbolicity:

$$(41) \qquad M > \sqrt{\frac{g(M_\infty)^2}{4 - \frac{\gamma-1}{2}g(M_\infty)^2}},$$

where

$$(42) \qquad g(M_\infty) = \frac{1 + \gamma M_\infty^2}{\frac{\gamma+1}{2}M_\infty\sqrt{1 + \frac{\gamma-1}{2}M_\infty^2}}.$$

The minimum M required for a locally hyperbolic equation is shown in figure 5. In case $g(M_\infty) > 2\sqrt{2/(\gamma-1)}$ such an M does not exist, i.e., the TSD can then not be hyperbolic. For $\gamma = \frac{7}{5}$ this leads to the condition $M_\infty \gtrsim 0.196$, recognized by the vertical asymptote in figure 5. For $M_\infty = 1$ the same hyperbolicity condition is encountered as for the Euler and FPE models, namely $M > 1$. It is important to note that formally inequality (41) is the condition numerical algorithms should use to determine if a central or upwind differencing scheme has to be used;

the widely used condition that locally $M > 1$, mentioned in e.g. [2], is a good approximation to (41) around $M_\infty = 1$.
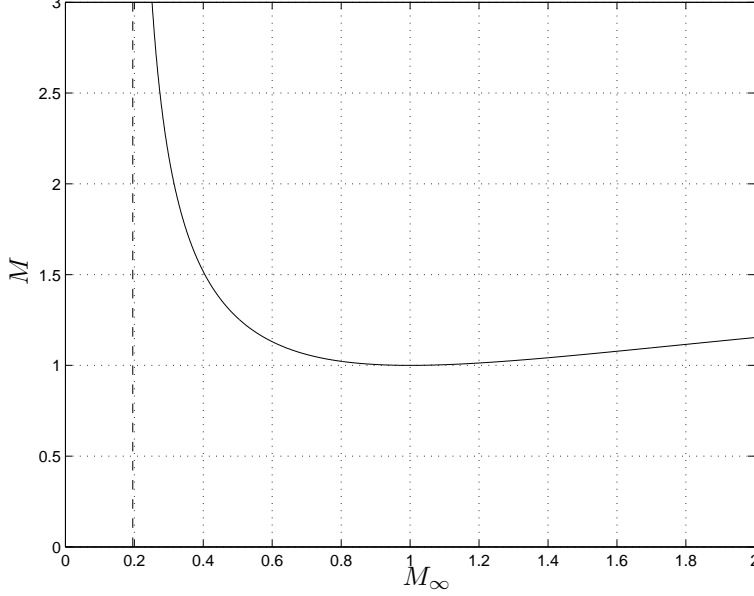

FIGURE 5. Minimum required M for a locally hyperbolic TSD as function of M_∞, $\gamma = \frac{7}{5}$.

To investigate the jump relations for the TSD, it is cast in the form of equation (2) by taking

$$(43) \qquad F = (1 - M_\infty^2)\varphi_x - \frac{\gamma + 1}{2} M_\infty^2 \varphi_x^2, \qquad\qquad G = \varphi_y.$$

Hence, following (20), the jump relation for a one-dimensional normal TSD shock reads

$$(44) \qquad \left[(1 - M_\infty^2)\varphi_x - \frac{\gamma + 1}{2} M_\infty^2 \varphi_x^2\right] = 0.$$

Rewriting gives

$$(45) \qquad \frac{1 - M_\infty^2}{\frac{\gamma+1}{2} M_\infty^2} = (\varphi_x)_2 + (\varphi_x)_1 = \frac{u_1 + u_2}{V_\infty} - 2.$$

$$(46) \qquad \boxed{\frac{M_1}{\sqrt{1 + \frac{\gamma-1}{2} M_1^2}} + \frac{M_2}{\sqrt{1 + \frac{\gamma-1}{2} M_2^2}} = \frac{1 + \gamma M_\infty^2}{\frac{\gamma+1}{2} M_\infty \sqrt{1 + \frac{\gamma-1}{2} M_\infty^2}}.}$$

Opposed to the Euler and FPE models, this normal shock relation for the TSD also depends on the free-stream Mach number M_∞. An explicit equation for M_2 can be obtained by rewriting equation (46) as

$$(47) \qquad M_2^{\text{TSD}} = \frac{f(M_1, M_\infty)}{\sqrt{1 - \frac{\gamma-1}{2} f(M_1, M_\infty)^2}},$$

where

$$(48) \qquad f(M_1, M_\infty) = g(M_\infty) - \frac{M_1}{\sqrt{1 + \frac{\gamma-1}{2}M_1^2}}.$$

So, in contrast to the FPE, a numerical method is not necessary to obtain M_2 as a function of M_1 and M_∞. Relation (46) has been plotted in figure 2 for different values of M_∞. It can be seen that only for $M_\infty = 1$ the TSD is a consistent approximation to the Euler equations near $M_1 = 1$, i.e., only for $M_\infty = 1$ it satisfies the trivial solution $M_1 = M_2 = 1$. For $M_\infty \neq 1$, one can observe the peculiar result that $M_2 > M_1$ for $M_1 = 1$. The aforementioned symmetry of the Euler and FPE relations around the line $M_2 = M_1$ still holds, but no longer around the point $M_2 = M_1 = 1$. Instead, the symmetry point is $(M_1, M_2) = (M^s, M^s)$, with M^s given by

$$(49) \qquad M^s = \sqrt{\frac{g(M_\infty)^2}{4 - \frac{\gamma-1}{2}g(M_\infty)^2}}.$$

For $M_\infty = 1$ this shift is zero and for all other M_∞ it is positive. We note that equation (49) is exactly equal to equation (41), allowing us to interpret the region $M_2 > M_1$ in figure 2 as a region where the TSD is not hyperbolic, so that solutions in this region are not valid shock solutions. Equation (16) shows that such solutions would correspond to unphysical expansion shocks.

A further, stricter, requirement on valid shock solutions comes from the denominator of (47). It is necessary that the term under the square root is positive, which gives the condition $M_\infty > M_\infty^*$ (there is no upper bound). In figure 6, M_∞^* is shown as a function of M_1, for $\gamma = \frac{7}{5}$. For this γ we find $M_\infty^*(M_1 = 1) \approx 0.294$ and $M_\infty^*(M_1 \to \infty) \approx 0.196$, the same value that was obtained from the requirement on hyperbolicity. In practice, flows with M_∞ close to M_∞^* would require strongly curved bodies or high angles of attack to be accelerated such that locally supersonic conditions appear. Since in such cases the small perturbation assumption underlying the TSD is not valid, the condition $M_\infty > M_\infty^*$ is not a serious limitation for practical flow problems with $\gamma = \frac{7}{5}$.

To investigate the accuracy of the TSD shock relation, we expand equation (46) in a series solution around $M_1 = 1$ and find (for convenience with $M_\infty = 1$):

$$(50) \qquad M_2^{\text{TSD}} = 1 - (M_1 - 1) + 3\frac{\gamma - 1}{\gamma + 1}(M_1 - 1)^2 + \mathcal{O}\left((M_1 - 1)^3\right).$$

The error in M_2 is again $\mathcal{O}\left((M_1 - 1)^2\right)$:

$$(51) \qquad M_2^{\text{Euler}} - M_2^{\text{TSD}} = \frac{2}{\gamma + 1}(M_1 - 1)^2 + \mathcal{O}\left((M_1 - 1)^3\right).$$

Compared to the FPE model, equation (26), near $M_1 = 1$ the error in the shock relation of the TSD at $M_\infty = 1$ and $\gamma = \frac{7}{5}$ is only slightly larger than for the FPE. This was already visible in figure 2. For mono-atomic gases ($\gamma = \frac{5}{3}$) and $M_\infty = 1$ comparison of (26) and (51) learns that the TSD is even slightly more accurate than the FPE.

An interesting case occurs when $M_\infty = M_1$; then TSD relation (46) yields:

$$(52) \qquad M_2^2 = \frac{2 + (\gamma - 1)M_1^2}{2\gamma M_1^2 - (\gamma - 1)}.$$

This expression is identical to relation (9) for the post-shock Mach number of the Euler equations. Graphically this is seen in figure 2 by the intersection of the TSD line at $M_\infty = 1.2$ with the Euler line at a value of $M_1 = 1.2$. Similarly, although not physical, the TSD line at $M_\infty = 0.8$ intersects the Euler line at $M_1 = 0.8$. The latter is not visible in figure 2, but due to the reversible nature of equation (46) (the symmetry with respect to $M_2 = M_1$), the TSD line at $M_\infty = 0.8$
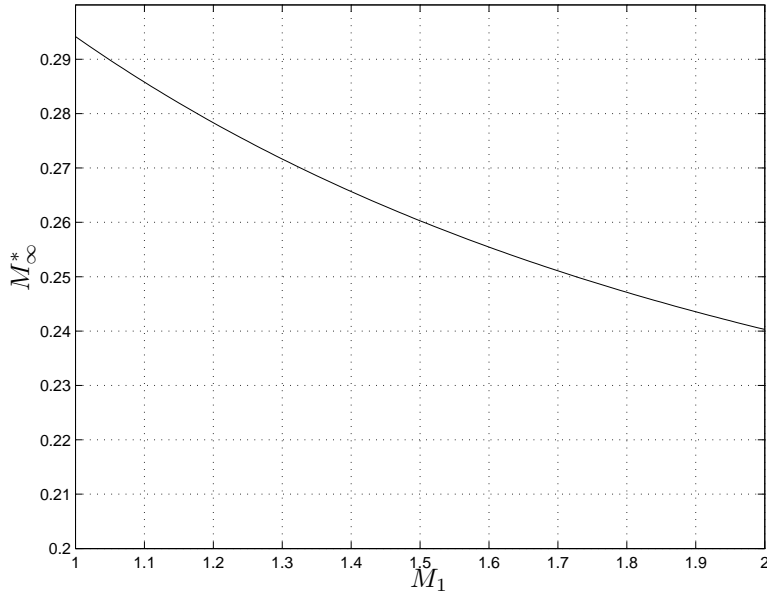
FIGURE 6. Minimum allowed free-stream Mach number versus pre-shock Mach number, $\gamma = \frac{7}{5}$.

also intersects at $M_2 = 0.8$, which is visible in figure 2. Although the jump in Mach number at $M_\infty = M_1$ matches the Euler jump, the pressure, density and temperature jumps do not, due to the fact that they are derived with the assumption of homentropic flow.

Shocks satisfying the TSD are again stronger than shocks satisfying the Euler equations if $M_\infty = 1$. For other M_∞ this is true only when $M_1 > M_\infty > 1$ or $M_2 < M_\infty < 1$.

The relative momentum error for the TSD is found by substituting M_2 according to equation (46) into equation (19). From figure 3 it is observed that the relative momentum error is rather insensitive to the free-stream Mach number. Substituting equation (50), including higher order terms, in equation (19) and Taylor expanding the result leads to:

$$(53) \qquad \frac{[p + \rho u^2]}{p_1 + \rho_1 u_1^2} = \frac{8}{3} \frac{\gamma(2\gamma - 1)}{(\gamma + 1)^3} (M_1 - 1)^3 + \mathcal{O}\left((M_1 - 1)^4\right).$$

The relative error in momentum conservation is of third order, as was the case for the FPE.

The TSD, as opposed to the FPE, also fails to conserve mass across shocks. For homentropic flows, the relative mass error can be written as

$$(54) \qquad \frac{[\rho u]}{\rho_1 u_1} = \left(\frac{1 + \frac{\gamma - 1}{2} M_1^2}{1 + \frac{\gamma - 1}{2} M_2^2}\right)^{\frac{\gamma + 1}{2(\gamma - 1)}} \frac{M_2}{M_1} - 1.$$

Looking at the full potential relation (23), it is confirmed that the relative mass error for the FPE is zero, as expected. Taylor expansion shows that

$$(55) \qquad \frac{[\rho u]}{\rho_1 u_1} = \frac{8}{3} \frac{2\gamma - 3}{(\gamma + 1)^2} (M_1 - 1)^3 + \mathcal{O}\left((M_1 - 1)^4\right),$$

so the relative mass error is third order, like the momentum and entropy error. In figure 7 the relative mass error according to TSD shock relation (46) is plotted as a function of M_1 for three different values of M_∞. There can be either mass gain, mass loss, or conservation of mass, depending on M_1 and M_∞. Points of zero relative mass error correspond to intersections of the TSD and FPE curves in figure 2. We note that, just as for the FPE, mass-conserving shocks do not necessarily give the best correspondence with experimental data.
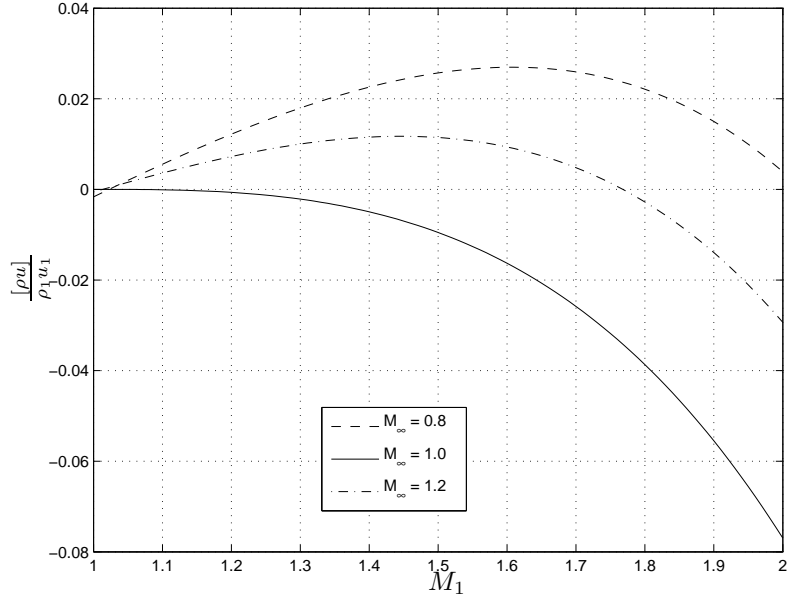

FIGURE 7. Relative mass error for the TSD, $\gamma = \frac{7}{5}$.

3.2. **Oblique shock relations.** The geometrical relation for oblique shocks, equation (31), is still valid. However, $\frac{u_2}{u_1}$ is not equal to $\frac{\rho_1}{\rho_2}$ anymore. Instead we can write

$$(56) \qquad \frac{u_2}{u_1} = \frac{M_{n,2}}{M_{n,1}} \sqrt{\frac{p_2}{p_1} \frac{\rho_1}{\rho_2}}.$$

Using the homentropic relations for the pressure ratio and density ratio across the shock, (56) can be rewritten as

$$(57) \qquad \frac{u_2}{u_1} = \frac{M_{n,2}}{M_{n,1}} \sqrt{\frac{1 + \frac{\gamma-1}{2}M_{n,1}^2}{1 + \frac{\gamma-1}{2}M_{n,2}^2}} = \frac{\tan(\beta - \theta)}{\tan\beta}.$$

By employing the same approach as in section 2.2, with now the TSD relation for the pre- and post-shock Mach numbers $M_{n,1}$ and $M_{n,2}$, the oblique shock relations for the TSD are added to figure 4. The jump in Mach number normal to the shock is the same as for the Euler equations if $M_{n,1} = M_{n,\infty}$, but the wave angle is not the same due to the assumption of homentropy. It can be seen that the FPE and TSD results are very close for $M_\infty = 1$, but for other M_∞ the results quickly diverge. For sufficiently high M_1 we can distinguish intersections with the TSD results.

4. Conclusion

In this paper an overview has been given of normal and oblique shock relations for Euler, full potential equation (FPE) and transonic small disturbance equation (TSD) flow models. Existing shock relations have been revisited and new shock relations have been derived, which are ideally suited for the verification of numerical methods. A novelty is that all relations are expressed in terms of pre- and post-shock Mach number only.

The normal shock relation for the FPE is an implicit relation between post- and pre-shock Mach numbers (M_2 and M_1) that has to be solved numerically. Compared to the Euler shock relations, it provides a second order approximation to M_2 in terms of $M_1 - 1$. The assumption of homentropy, a third order error in terms of $M_1 - 1$, leads to a gain in momentum across the shock, which is also a third order error term.

For the TSD an explicit expression is derived for M_2 in terms of M_1 and free-stream Mach number M_∞. For general M_∞ this is an inconsistent approximation to the Euler expressions for M_2, i.e., solutions do not pass through $M_1 = M_2 = 1$, although the associated error is small for M_∞ near 1. The switch from elliptic to hyperbolic is not at $M = 1$ (except for $M_\infty = 1$), but at a higher value. This value should be used in numerical codes when locally a switch between differencing schemes is used. As for the FPE, an error in momentum conservation is present, but additionally an error in mass conservation is introduced. Certain values of M_∞ deserve special attention:

(1) In case M_∞ is too small (e.g. smaller than ~ 0.294 for $M_1 = 1$ and $\gamma = \frac{7}{5}$) the TSD shock relations become invalid.
(2) In case $M_\infty = 1$, the TSD expression for M_2 is consistent, second order accurate in $M_1 - 1$ and the associated errors in mass and momentum are both third order in terms of $M_1 - 1$. It is very close to the FPE expression, and for certain γ, e.g. mono-atomic gases with $\gamma = \frac{5}{3}$, it is even more accurate.
(3) In case $M_\infty = M_1$ no approximation is involved since the expression for M_2 of the Euler equations is recovered.
(4) For certain combinations of M_1 and M_∞ the TSD shock relations are equal to the FPE shock relations, and there is no mass conservation error.

Oblique shock relations have also been derived for both the FPE and TSD model. As for Euler flows, the relations allow for computations of the shock-wave angle (if existent), for known pre-shock flow, deflection angle, and free-stream Mach number in case of the TSD model. For small deflection angles and small upstream Mach numbers the FPE gives a good approximation to the oblique shock relations obtained from the Euler equations. This remains true for the TSD if M_∞ is close to unity.

References

[1] M. Hafez and E. Wahba. Numerical simulations of transonic aerodynamic flows based on a hierarchical formulation. *International Journal for Numerical Methods in Fluids*, 47:491–516, 2005. doi:10.1002/fld.827.

[2] T.L. Holst. Transonic flow computations using nonlinear potential methods. *Progress in Aerospace Sciences*, 36:1–61, 2000. doi:10.1016/S0376-0421(99)00010-X.

[3] T.L. Holst. Transonic flow potential method development at Ames Research Center. *Computers & Fluids*, 38(3):482–490, 2009. doi:10.1016/j.compfluid.2008.06.011.

[4] G.H. Klopfer and D. Nixon. Nonisentropic potential formulation for transonic flow. *AIAA Journal*, 22(6):770–776, 1974.

[5] W.H. Mason. On the use of the potential flow model for aerodynamic design at transonic speeds. In *33rd Aerospace Sciences Meeting & Exhibit*, January 1995. Reno, NV, AIAA Paper 95-0741.

[6] J.L. Steger and B.S. Baldwin. Shock waves and drag in the numerical calculation of isentropic transonic flow. Technical Report TN D-6997, NASA, 1972.

[7] J. van der Vooren and J.W. Slooff. On inviscid isentropic flow models used for finite difference calculations of two-dimensional transonic flows with embedded shocks about airfoils. Technical Report MP 73024 U, NLR, 1973.